Amplitude Responses of a Square Cylinder undergoing Vortex-Induced Vibrations in the Laminar Regime

F. Tong[1], L. Cheng[1, 2], M. Zhao[3] and H. An[1]

[1] School of Civil, Environmental and Mining Engineering
The University of Western Australia, 35 Stirling Highway, Crawley, WA 6009, Australia

[2] State Key Laboratory of Coastal and Offshore Engineering,
Dalian University of Technology, Dalian, 116024, China

[3] School of Computing, Engineering and Mathematics,
University of Western Sydney, Locked Bag 1797, Penrith NSW 2751, Australia

Abstract

This paper presents a numerical study on the vortex-induced vibrations (VIV) of a square cross-section cylinder in the steady current. A new branch of high amplitude of responses (HB) was observed in the laminar regime, in agreement with a handful studies on the topic. In addition, this new branch is found to be dependent on several controlling parameters, including the approaching direction of the flow relative to the square cylinder, the Reynolds number (Re), the mass ratio, as well as the number of degree-of-freedom. In the laminar flow regime, it is found this new branch only occur when Re is greater than a critical value and only when the vibration of the square cylinder is two-degree-of-freedom. The range of reduced velocity where the HB regime occurs strongly depends on above listed parameters.

Introduction and Motivation

When a bluff body is placed in a steady flow, the vortex shedding leads to periodic fluid forces on the body in both in-line and transverse directions of the incoming flow. If the bluff body is mounted elastically, these periodic forces may induce large amplitude of vibrations to the structure. This phenomenon of flow-induced vibration (FIV) is generally termed as vortex-induced vibration (VIV). From engineering application point of view, ocean currents can induce vibrations of offshore pipelines, risers and platforms, and wind can trigger vibrations of chimneys, skyscrapers and hanging lines. For this reason, extensive studies of VIV of circular cylinders has been performed in the past a few decades [2, 11].

Dynamics of response

Figure 1 shows a sketch of a square cylinder with a side length of D and a mass of M placed in fluid flow with a velocity of U_∞ and density of ρ. The structure is subjected to forces (F) induced by the fluid. A coordinate system is defined with the x-direction pointing the incoming flow direction. The non-dimensional equation of motion of the cylinder is expressed as,

$$M^* \frac{\partial^2 X_i^*}{\partial t^{*2}} + C^* \frac{\partial X_i^*}{\partial t^*} + K^* X_i^* = F_i^* \qquad (1)$$

where a variable without and with a superscript "*" stands for dimensional and non-dimensional values, respectively. Here, t is the time, $X^*=X_i/D$ is the displacement of the cylinder in either in-line (x-) and transverse (y-) directions, $t^*=tU/D$ is the time, $M^*=M/(\rho D^2)$ is the mass, $C^*=C/(\rho U_\infty D)$ is the damping coefficient, $K^*=K/(\rho U_\infty^2)$ is the stiffness and $F_i^*=F_i/(\rho U_\infty^2 D)$ is force on the cylinder.

The reduced velocity (V_r) is introduced in the study of VIV, which is defined as

$$V_r \equiv \frac{U_\infty}{f_n D}, \qquad (2)$$

where $f_n = \sqrt{K/M}/2\pi$ is the natural frequency. Also, we will use $m_r = M^*$, to represent reduced mass.

The fourth independent parameter of the problem is the Reynolds number, $Re = U_\infty D/\nu$. In the present paper, D is used in this definition irrespective of the flow approaching angle α.
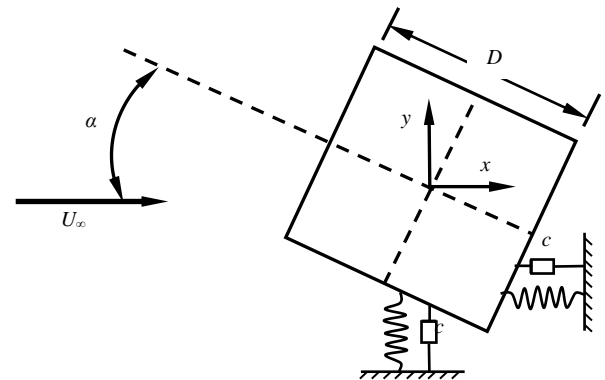

Figure 1 Schematic representation of the vortex-induced vibration of a square cross-sectional cylinder in steady flow, subjected to variable angles of attack and two-degree of freedom.

Previous studies

The VIV response of a circular cylinder of low mass-damping parameter ($m_r\zeta$) was classified into four regimes with the increase of V_r, namely, the initial excitation branch (IB), the upper branch (UB), the lower branch (LB) and the desynchronization [5, 7-9]. In the case of high $m_r\zeta$, only three regimes (i.e., IB, UB and desynchronization) present [4]. In each regime, the vibration behaves differently in both amplitude and frequency. It is worthwhile to mention that although studies leading to the classification of response regimes were carried out at approximately $Re\sim10^4$, similar vibration responses and flow features were reproduced at the laminar regime with two-dimensional (2-D) numerical simulations [1, 13]. However, the UB is not as clear in the laminar flow.

On the other hand, a bluff body with square cross-section represents the simplest setups considering oblique flow angles of attack, sharp corners and some afterbody (the part of body after separation points) in the study of FIV [15]. The geometry matters in the study of FIV and when it comes to a square cylinder, the main purpose of much published work usually is to investigate

the galloping phenomena along with VIV, since it is one of the simplest geometries that can gallop.

One of the most interesting discoveries of recent research on a square cylinder undergoing FIV is a new response branch at some asymmetric orientations, reported independently in two studies, i.e., Nemes *et al.* [11] in laboratory experiments at $Re \sim 10^4$ and Zhao *et al.* [16] in numerical study at $Re=100$. The amplitude of response in the new branch exceeds the ones in the traditionally lock-in regime in the UB. Nemes *et al.* [11] referred to this new branch as higher branch (HB). It appears the HB only occurs at intermediate alignment angles where no galloping is observed, and gradually disappears with increasing flow attacking angle when the mechanism of VIV takes over.

By using two-dimensional (2-D) numerical simulations, this paper focus on the dependence of the higher branch on four different parameters, including the angles of attack, the degree-of-freedom, the mass ratio and the Reynolds number. Simulations were carried out in the laminar flow regime, where 2-D numerical study is sufficient and also the VIV can be studied in isolation from galloping for the square cylinder.

Numerical method

The motion of the fluid is computed by the two-dimensional incompressible Navier–Stokes (NS) equations in a moving reference frame attached to the cylinder, which is realized by introducing an extra forcing term into the momentum equation [12]. The NS equations are solved using Nektar++, an open-source software framework [3]. A high-order finite element method of spectral/hp element method was employed in solving the NS equations in conjunction with a second-order time-splitting scheme and a quadrilateral spectral element-Fourier expansion in the spatial discretization [6].

A square computational domain was employed in the numerical simulations. At the left, top and bottom boundaries the velocity were set to $u = U + u_{cyl}$ and $v = v_{cyl}$, where (u_{cyl}, v_{cyl}) are the cylinder velocity as a result of VIV in the x- and y-directions, respectively. On the cylinder surface, the no-slip condition was imposed, while the normal velocity gradient on the right (outlet) boundary is set to zero. The pressure was fixed to zero at the outlet, and the pressure gradient on the wall and at the far-field boundaries was dealt with using higher-order boundary conditions [6].

Initial tests were aimed at assessing the domain size and mesh dependency and the validity of the numerical model were carefully performed; after that a domain of $x \times y = 65D \times 40D$ was chosen, which leads to a blockage ratio of 2.5%.
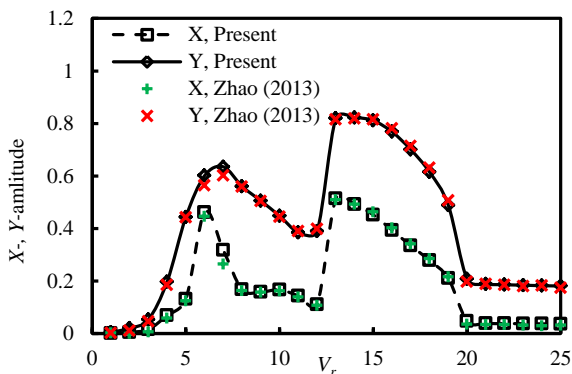

Figure 2 Numerical validation on the vibration amplitudes of a square-cross-sectional cylinder in steady flow at $Re=100$, $m_r = 3$ and $\alpha = 22.5°$.

The 2DoF VIV of a square cylinder with an attacking angle of 22.5° is simulated and the amplitudes of displacement in the x-direction (X-amplitude) and y-direction (Y-amplitude) are compared to those from Zhao *et al.* [16] in Figure 2. It is seen that the two sets of data agree well with each other. The Y-amplitude is consistently larger than X-amplitude across the investigated V_r, which is thought due to difference in the vibration amplitudes of forces in the two directions. There are two regimes of high amplitude responses with the increase of V_r from 1 to 25. The maximum amplitudes in both directions at higher V_r are greater than those at the low V_r.

Result Discussion

A number of simulations were carried out to investigate the influences of four parameters to the response of the square cylinder in the laminar regime, including angles of attack ($\alpha \in$ [0°, 45°]), degree-of-freedom (1DoF in the y-direction or 2DoF in both x- and y-direction), mass ratio ($m_r \in$ [0.1, 30]) and Reynolds number ($Re \in$ [60, 160]), which will be discussed separately.
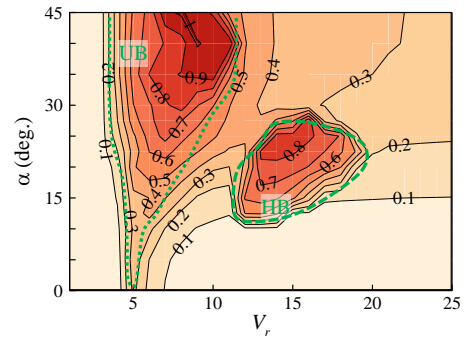

Figure 3 Vortex-induced-vibration responses of a square cylinder as a function of reduced velocity (V_r) and angles of attack (α) at $Re = 100$ and $m_r = 3$. Two regimes of high amplitude of responses are approximately marked.

Influence of α

A global view of the amplitude of the response in the y-direction in the (V_r, α)-space for 2DoF VIV of a square cylinder at $Re=100$ and $m_r = 3$ is presented in Figure 3 as a contour map. The maximum amplitude locates at (V_r, α) = (8, 45°) at 1.02. A prominent feature is that there are two regimes of large amplitude in the map. The first regime locates at lower reduced velocity at $V_r \in$[4, 10] for all angles of attack, while the second at higher reduced velocity around $V_r \in$ [11, 17] for $\alpha \in$ [12.5°, 27.5°]. Following the nomenclatures by Morse and Williamson [10] and Nemes *et al.* [11], these regimes of high-amplitude vibrations are named as UB and HB, respectively. Compared with the map of amplitude of response in 1DoF study at $Re \sim O(10^3 \sim 10^4)$ from Nemes *et al.* [11], no galloping phenomenon is observed in the laminar regime. Another major difference to the map at $Re \sim O(10^3 \sim 10^4)$ is that the HB regime has been shifted to larger angles of attack at $\alpha \in$ [12.5°, 27.5°]. Considering the large difference in Re and the number of DoF of the present map to that of Nemes *et al.* [11] though, the similarity in the maps of amplitude response is remarkable.

It is observed in Figure 3 that for any fixed angle of attack, if HB occur, the highest Y-amplitude always falls into the HB regime. However globally, the maximum Y-amplitude locates at the largest attacking angle in the UB regime. In both UB and HB regimes, it is generally true that the maximum Y-amplitude grows when α is increased. For the range of V_r when lock-in occurs, it is seen that the UB regime widens significantly with the increase of α; while on the other hand, the range of V_r over which HB occurs maximizes at $\alpha = 22.5°$, from $V_r = 13$ to 19.

While it is not shown here, but the regimes of X-amplitude response is similar to that of Y-amplitude with two clear regimes

of large amplitude of responses, only for every angle of attack the Y-amplitude is much larger than the X-amplitude, which peaks at the UB regime at just over $0.5D$. For the majority of the cases, the large amplitude of responses in x-direction coincides in similar V_r with that in the y-direction.
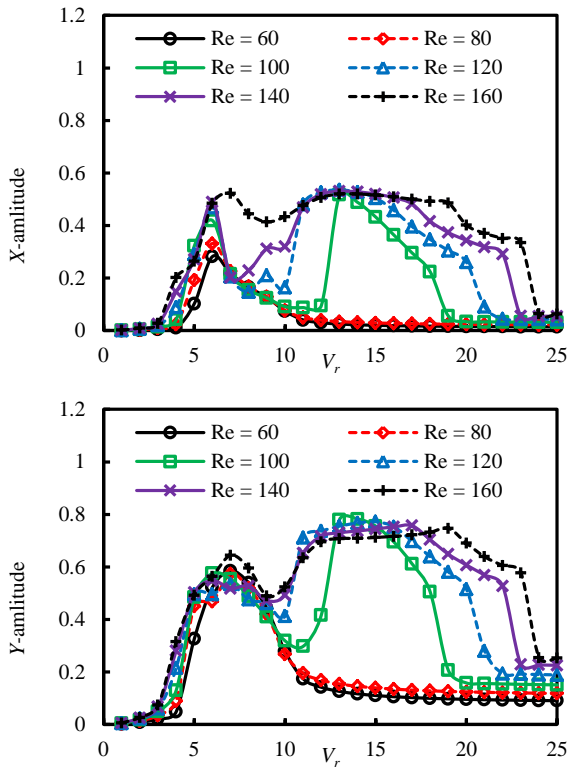

Figure 4 Comparison on the vibration amplitudes of a square-cross-sectional cylinder in steady flow at m_r=3 and $\alpha = 20\,°$ at six selected Reynolds number (Re).

Influence of Re

Figure 4 compares the vibration amplitudes from 2DoF study at $m_r = 3$ at six Reynolds numbers in the range of $Re \in [60, 160]$. It was found that the HB regime in both directions is highly dependent on Re, especially when it is compared to the UB regime. It is observed that no HB regime occurs at $Re = 60$ and 80, while the range of V_r for HB regime widens greatly with the further increase of Re from 100. At $Re = 160$, the range of V_r for regimes of UB and HB in both directions tends to connect together and thus the response amplitudes are high in the range of $V_r = 5$ to 23, only with comparatively small amplitude at around V_r=10. On the contrary, the Reynolds number has little effect on the UB regime. The UB regime occurs at around $V_r = 6$ and the range of V_r of the UB regime in the y-direction is slightly wider than that in the x-direction. The range of V_r for HB regime is much wider than that of UB regimes at any Re when HB does occur, which is especially true for the Y-amplitude response.

The amplitude responses in the two directions behave slight differently. In the UB regime, the maximum X-amplitude increases about 60% with the increase of Re, from 0.33 at $Re = 60$ to 0.52 at $Re = 160$, whereas the Y-amplitude only varies in the range of 0.52 to 0.64. On the other hand in the HB regime, the maximum amplitude seems quite independent from the change of Re, which occurs at V_r around 13~16 for both X- and Y-amplitude, at $0.52D$ and $0.77D$, respectively.

The dependence of amplitude response to Re is believed to be due to the characteristics of vortex shedding at these Re, where a detailed observation on the vibration frequency and flow field is thought to be helpful in providing the explanation.

Influence of Mass ratio

The mass ratio also plays a significant role in VIV responses of a square cylinder, as that for a circular cylinder. Figure 5 illustrates the boundary of reduced velocities, within which (shaded areas) the UB and HB regimes are observed for a range of mass ratios at fixed Re=100 and $\alpha = 20\,°$, along with the maximum amplitude of response in each regime.
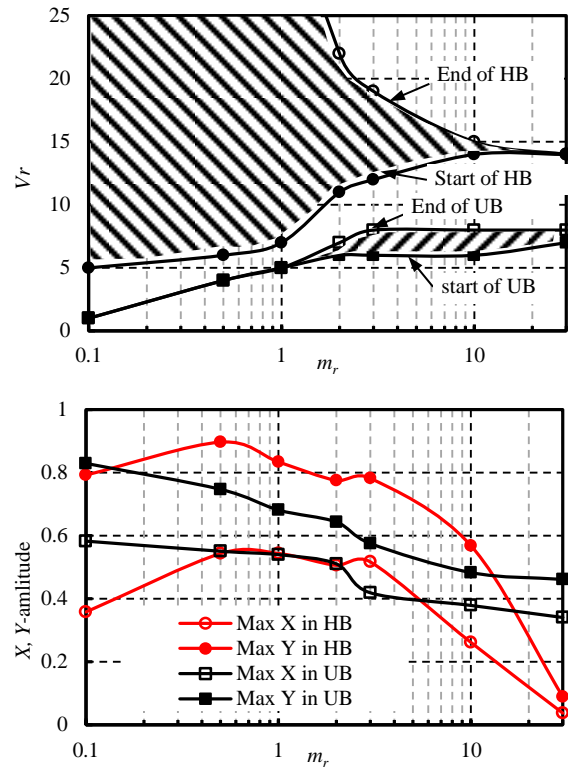

Figure 5 The variations of Upper branch (UB) and high branch (HB) amplitude responses of a square cylinder in steady flow at Re=100 and $\alpha = 20\,°$.

It is observed the HB regime dominates light square cylinder, with much wider range of V_r for $m_r < 1$, where only a single case of UB is observed in a V_r resolution of 1. Similar to that of a circular cylinder, there seems to be a critical value of m_r, lower than which an unbounded (with regard to V_r) HB synchronization regime occurs. This critical value falls smaller than $m_r = 1$, which is 0.54 for a circular cylinder [14]. The area of HB regimes shrinks greatly with increase of m_r over $m_r \geq 2$, while that for the UB sees much less change. From $m_r = 10$ onwards, the range of V_r of UB regime overtakes that of HB regime and at $m_r = 30$, only a single case of HB regime is observed.

For the maximum amplitude of response, it behaves quite differently in the two regimes. In the UB regime, both X- and Y-amplitude experience a steady, 40% drop with the increase of m_r from 0.1 to 30. However, the amplitudes in the HB regime increase slightly before a more than 90% plunge in the same range of m_r. At both end of investigated m_r in the present paper, the amplitude of response in HB regime is actually smaller than that in UB regime, in contrast to those discussed above and in published studies [11, 15], This demonstrates that the amplitude in the HB regime does not necessarily Higher than the amplitude in the UB regime.

Influence of number of the DoF

It is observed that the large amplitude of HB regime totally disappears in the laminar regime when the square cylinder is only allowed to move in the transverse direction (1DoF). This is

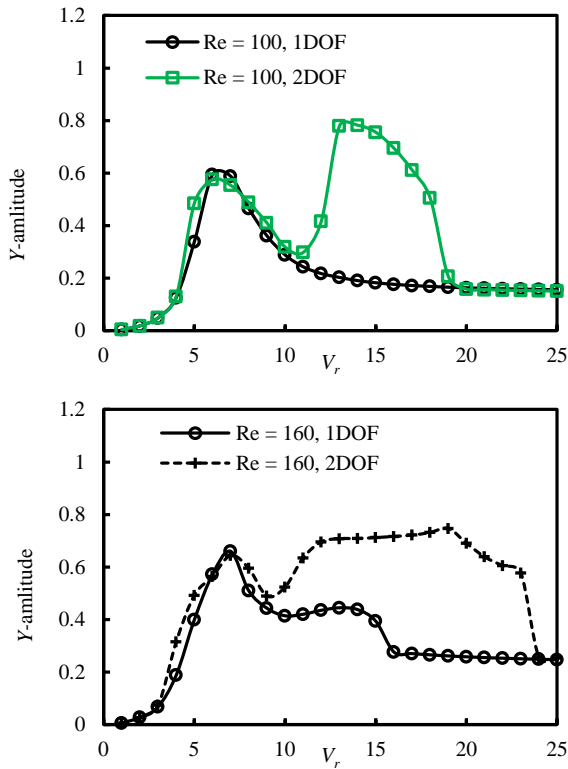distinctly different from what was observed in high *Re* experimental studies [11, 15].

Figure 6 Comparison on the vibration amplitudes of a square-cross-sectional cylinder in steady flow at *Re*=100 and 160 with m_r = 3 and α = 20°.

Both 1DoF and 2DoF studies were carried out in the range of *Re* = 100 ~ 160. Figure 6 shows the comparison between the *Y*-amplitude responses from 1DoF and 2DoF simulations. For the UB regime, only a slight change in *Y*-amplitude is observed in the simulations, while the range of V_r of UB regime sees even less dependency.This is similar to the studies on a circular cylinder that the number of DoF does not bring much influence on the amplitude response.

Surprisingly, no HB is observed when the square cylinder is restricted to move in the *y*-direction in the laminar regime, while the HB regime has been observed in 1DoF experimental study at $Re \sim O(10^3 \sim 10^4)$. This comparison suggests that in 1DoF VIV, the HB can only occur for *Re* larger than a critical *Re*, which is apparently larger than 160.

Conclusions

Vortex-induced vibrations (VIV) of a square cross-section cylinder in steady current in the laminar regime was numerically studied. The amplitude responses are presented with a wide range of controlling parameters.

1. A new branch of high amplitude of responses (HB) is confirmed in the laminar regime;
2. This new branch is found to be dependent on several controlling parameters, including direction of the flow with regard to the arrangement of the square cylinder, the Reynolds number (*Re*), the mass of the cylinder as compared to the fluid, as well as the numbers of degree-of-freedom. Generally, light cylinder with low mass ratio and high *Re* encourage the generation of HB.
3. This new branch only occur when *Re* is greater than a critical value and only in the situation of two-degree-of-freedom in the laminar regime. When HB regime does occur, the range of reduced velocity for HB regime also depends greatly on a number of parameters.

References

[1] Blackburn, H. and Henderson, R., Lock-in behavior in simulated vortex-induced vibration. *Experimental Thermal and Fluid Science*. **12**(2), 1996, 184-189.

[2] Blevins, R.D., Flow-induced vibration. 1990.

[3] Cantwell, C.*, et al.*, Nektar++: An open-source spectral/hp element framework. *Computer Physics Communications*. **192**, 2015, 205-219.

[4] Feng, C., The measurement of vortex induced effects in flow past stationary and oscillating circular and d-section cylinders. *Retrospective Theses and Dissertations, 1919-2007*, 1968.

[5] Govardhan, R. and Williamson, C., Modes of vortex formation and frequency response of a freely vibrating cylinder. *J. Fluid Mech.* **420**, 2000, 85-130.

[6] Karniadakis, G.E., Israeli, M., and Orszag, S.A., High-order splitting methods for the incompressible Navier-Stokes equations. *J. Comput. Phys.* **97**(2), 1991, 414-443.

[7] Khalak, A. and Williamson, C., Dynamics of a hydroelastic cylinder with very low mass and damping. *J. Fluids Struct.* **10**(5), 1996, 455-472.

[8] Khalak, A. and Williamson, C., Fluid forces and dynamics of a hydroelastic structure with very low mass and damping. *J. Fluids Struct.* **11**(8), 1997, 973-982.

[9] Khalak, A. and Williamson, C., Motions, forces and mode transitions in vortex-induced vibrations at low mass-damping. *J. Fluids Struct.* **13**(7), 1999, 813-851.

[10] Morse, T. and Williamson, C., Prediction of vortex-induced vibration response by employing controlled motion. *J. Fluid Mech.* **634**, 2009, 5-39.

[11] Nemes, A.*, et al.*, The interaction between flow-induced vibration mechanisms of a square cylinder with varying angles of attack. *J. Fluid Mech.* **710**, 2012, 102-130.

[12] Newman, D.J. and Karniadakis, G.E., A direct numerical simulation study of flow past a freely vibrating cable. *J. Fluid Mech.* **344**, 1997, 95-136.

[13] Prasanth, T. and Mittal, S., Vortex-induced vibrations of a circular cylinder at low Reynolds numbers. *J. Fluid Mech.* **594**, 2008, 463-491.

[14] Williamson, C.H.K. and Govardhan, R., Vortex-induced vibrations. *Annu. Rev. Fluid Mech.* **36**, 2004, 413-455.

[15] Zhao, J.*, et al.*, Fluid–structure interaction of a square cylinder at different angles of attack. *J. Fluid Mech.* **747**, 2014, 688-721.

[16] Zhao, M., Cheng, L., and Zhou, T., Numerical simulation of vortex-induced vibration of a square cylinder at a low Reynolds number. *Phys. Fluids*. **25**(2), 2013, 3603.